

Syngas production by electrochemical CO₂ reduction in an ionic liquid based-electrolyte



Tiago Pardal^{a,1}, Sofia Messias^a, Margarida Sousa^a, Ana S. Reis Machado^{a,*},
Carmen M. Rangel^b, Daniela Nunes^c, Joana V. Pinto^c, Rodrigo Martins^c,
Manuel Nunes da Ponte^c

^a Omnidea, Lda, Travessa António Gedeão, No. 9, 3510-017 Viseu, Portugal

^b Laboratório Nacional de Energia e Geologia, Estrada do Paço do Lumiar, 22, 1649-038 Lisboa, Portugal

^c LAQV, REQUIMTE, Departamento de Química, Faculdade de Ciências e Tecnologia, Universidade Nova de Lisboa, 2829-516 Caparica, Portugal

ARTICLE INFO

Article history:

Received 29 November 2016

Received in revised form 5 January 2017

Accepted 11 January 2017

Available online xxx

Keywords:

Carbon dioxide

Syngas

Electroreduction

Ionic liquids

Copper–zinc alloys

ABSTRACT

The electrochemical reduction of carbon dioxide dissolved in a solution of water and ionic liquid as electrolyte, at high-pressure and near room-temperature, is reported. This work describes an electro-deposition strategy for the preparation of copper substrate cathodes, coated with bimetallic zinc–copper films, obtained from deep-eutectic solvents plating baths. The prepared bimetallic cathodes showed electrochemical activity for syngas production in 1-butyl-3-methylimidazolium triflate, with yields of 85 NμL (normal microliter) cm⁻² C⁻¹/170 NμL cm⁻² h⁻¹, high selectivities, tunable H₂/CO ratio and low energetic requirements.

© 2017 Elsevier Ltd. All rights reserved.

1. Introduction

In general electrochemical processes, offer good reaction selectivity and reduced cost, because of the possibility of direct control of electrode surface free energy through electrode potential. These processes are sustainable only when electricity is obtained from renewable sources. The intermittent nature of these energy sources requires the capacity for large-scale electricity storage. This work reports the development of a low temperature process (near room temperature) for producing non-fossil syngas by co-electrolysis of CO₂ and water that has the potential to achieve this goal.

Syngas is a very valuable and versatile energy carrier. It can be converted into easily stored and transported liquid fuels by the well-established Fischer-Tropsch technology [1]. It can be produced from any hydrocarbon feedstock, natural gas, naphtha, residual oil, petroleum coke, coal, and biomass. All these processes have in common the use of high temperatures, well above 100 °C. At present, syngas is mainly produced from steam reforming of natural gas. Despite this being a mature technology, processes for

syngas production using several feedstocks are being actively investigated to increase their efficiency and lower their production cost [2,3].

Electrochemical carbon dioxide reduction into chemicals, such as fuels, has been actively investigated due to its potential for converting waste CO₂ captured from industrial emissions into carbon neutral products. However, due to the extreme stability of the CO₂ molecule, the potential that is necessary to apply for CO₂ electrochemical reduction in water at 25 °C, at atmospheric pressure is high: −1.9 V vs. SHE, because the first electron reduction involves the bending of the linear CO₂ molecule to form the [[•]CO₂]⁻ radical anion [4]. Therefore, the energy required for the process is usually high, and the energy efficiency as well as yield of the desired product are generally low [5].

Zhao et al. [6] used for the first time room temperature ionic liquids (ILs) as electrolytes for the electrochemical reduction of high-pressure CO₂, without other carbon-based reagents, due to their wide electrochemical windows, high solubility for CO₂ and reasonably good intrinsic ionic conductivities.

Room temperature ILs are generally defined as organic salts that are liquid at temperatures below 100 °C. The capability of ionic liquids to absorb CO₂ both physically [7] and chemically [8] opens-up the possibility of simultaneous capture and conversion CO₂ into valuable chemical products. Following the pioneer work of Zhao

* Corresponding author.

E-mail address: authors@omnidea.net (A.S. R. Machado).

¹ Institutional correspondence.

et al. other researchers have used ILs as an additive to the electrolyte [9,10].

In this context, Alvarez-Guerra et al. published a comprehensive review that includes the use of ILs in electrosynthesis of valuable compounds, using CO₂ as a reactant, and in the electrochemical reduction of CO₂ without other carbon-based reactants [11]. This review work clearly shows the important role of certain imidazolium-based ILs in lowering the overpotential of electrochemical CO₂ reduction. Rosen et al. [12] used a silver working electrode to reduce CO₂ to CO at atmospheric pressure in a hydrated IL 1-ethyl-3-methylimidazolium tetrafluoroborate (EMIMBF₄), where water was the proton source at overpotentials as low as 0.2 V with Faradaic efficiencies higher than 96%. This study also showed that the ionic liquid lowers the energy of the [CO₂]⁻ intermediate thereby decreasing the initial barrier to reduction. Di Meglio et al. [9] have reported that an economical bismuth-based material could promote the electrochemical conversion of CO₂ to CO at overpotentials below 0.2 V operating with a Faradaic efficiency of approximately 95%. CO₂ saturated acetonitrile containing millimolar concentrations of a 1,3-dialkyl substituted imidazolium based ionic liquid promoter such as 1-butyl-3-methylimidazolium triflate ((BMIM)OTf) was used as electrolyte. Zhang et al. [13] have demonstrate the effect of Bi catalyst's size and surface condition for an efficient organic phase CO₂ conversion to CO. Medina-Ramos et al. [10] showed that electrochemically prepared Bi and Sn catalysts were highly active, selective and a robust platform for CO evolution, with partial current densities of 5–8 mA cm⁻² at applied overpotentials <0.25 V in the presence of (BMIM)OTf in acetonitrile solutions. By contrast, electrodeposited Pb and Sb catalysts do not promote rapid CO generation with the same level of selectivity. The Pb-material is only approximately 10% as active as the Sn and Bi systems at an applied potential of -1.95 V and is rapidly passivated during catalysis. Watkins et al. [14] used an aqueous solution of 1-ethyl-3-methylimidazolium trifluoroacetate (EMIMTFA) for the direct reduction of carbon dioxide into formate at indium, tin, and lead electrodes; yields of ca. 3 mg h⁻¹ cm⁻² were obtained. Product selectivity was observed upon changing the IL anion. In EMIM based ILs on Pb electrodes oxalate formation is favoured in the presence of Bis(trifluoromethylsulfonyl)imide (NTF₂), whereas formate formation is favoured when trifluoroacetate (TFA⁻) is used as referred above [15]. Barrosse-Antle et al. [8] studied CO₂ electrochemical reduction in 1-butyl-3-ethylimidazolium acetate observing that CO₂ electrochemical reduction was not sustainable, because CO₂ is almost irreversible chemically absorbed. Hollingsworth et al. used a hydrated (0.7 mol L⁻¹ H₂O) 0.1 mol L⁻¹ trihexyltetradecylphosphonium 1,2,4-triazolide, [P66614] [124Triz] solution in acetonitrile to reduce CO₂ at Ag, Au and Pt electrodes. This ionic liquid has been shown to chemisorb CO₂ through equimolar binding of the carbon dioxide with the 1,2,4-triazolide anion [16,17], favouring formate formation by a low energy route (-0.7 V vs. Ag/AgNO₃ with 95% Faradaic efficiency in formate on Ag electrodes). Thus, literature shows that the main products from CO₂ reduction in IL-based electrolytes are CO and formate. To our best knowledge there are only three works that report syngas production, the work of Zhao et al. [6] the work of Asadi et al. [18] in which the control of the H₂/CO ratio is achieved by the tuning of applied potential and the work of Liu et al. [19] in which the control of the H₂/CO ratio is achieved by manipulation of the pH on either side of an anion exchange membrane, as well as the use of bimetallic Ag/Ni catalysts on the cathode. In the former work, supercritical CO₂ and water were electrolyzed at a copper cathode in the hydrophobic ionic liquid, 1-*N*-butyl-3-methylimidazolium hexafluorophosphate (BMIMPF₆), using a platinum anode. The electrolysis products detected were CO, H₂, and traces

of formic acid. However, large overpotentials were required for carrying out electrochemical reduction.

In the majority of systems using ionic liquid-based electrolytes, H₂ production is suppressed due to the cation forming a monolayer on the electrode surface [20] and CO is mainly produced, the tunability of H₂/CO is very limited, or the selectivity for syngas is poor. In conventional aqueous-based electrolytes hydrogen evolution is a strong competing reaction and generally electrocatalytic systems are not selective for syngas, or produce mainly CO (H₂/CO ratios near zero) [21]. Thus, flexible processes that can produce syngas with a tunable H₂/CO ratio are needed.

Pressure is a process parameter influencing significantly many chemical systems. As implementing systems that work above atmospheric pressure is not as straightforward as operation at atmospheric pressure, this parameter is often not studied. A limited number of studies employing high-pressure for the electrosynthesis of valuable compounds using CO₂ as a reactant that involve the use of ILs have been reported [11], namely, Hiejima et al. [22] studied the electrosynthesis of 2-phenylpropionic acid from CO₂ and found out that current efficiency that was low under ambient conditions, drastically increased with temperature and pressure, which was mainly explained by the increase of the diffusion coefficient of the reactant in the IL.

Current density and selectivity of the CO₂-water co-electrolysis was also found to be dependent on pressure [21]. To our best knowledge, there is only one study that was carried out at high-pressure using an ionic liquid based-electrolyte [6]. In fact, high-pressure CO₂ reduction stands out as being one of the most promising methods for achieving a commercial electrochemical process, as it was demonstrated that current densities of 3 A cm⁻² could be obtained, using an aqueous phosphate buffer electrolyte [23]. Current densities of this order of magnitude were only recently reported for high temperature (~800–900 °C) solid oxide electrolyzers [24,25].

To design a commercial semi-continuous or continuous high-pressure process for CO₂ electrochemical reduction is a challenging task. Reactants must be fed through gas-tight fittings rated for high pressure and products removed also through gas-tight fittings. Electric insulation of the electrochemical reactor must be accomplished. The pressure of the system must be controlled, so that a pressure difference between the cathodic and anodic compartment of the flow cell doesn't arise, which would cause the burst of the separator. Alternatively, an ionic conducting material with a suitable pressure rating would have to be used, or developed for the separator. This work reports a first development phase in which a single compartment high-pressure electrochemical cell was used and the experiments were carried out in batch mode, under CO₂ static pressure. The use of a single compartment high-pressure electrochemical cell presents also its difficulties. The use of a noble metal anode, such as Pt, may cause the oxidation of the products produced at the cathode, or can be poisoned [12] by the CO arising from CO₂ reduction. The use of a sacrificial anode may contaminate the electrolyte producing the correspondent cations that can be subsequently electrodeposited at the cathode.

Katoh et al. studied the electrochemical reduction of CO₂ by bimetallic Zn-Cu cathodes in aqueous 0.05 M KHCO₃ electrolytes at atmospheric pressure and 2 °C [26]. These researchers observed partial current densities for CO of less than 1 mA/cm². The use of bimetallic Zn-Cu cathodes coupled with ionic liquid-based electrolytes has not yet been reported. This work reports results of the development of electro-catalysts made-up of abundant common metals (Cu and Zn) and of a process for the production of syngas from CO₂ with a controlled H₂/CO ratio by tuning the catalyst composition by electrochemical reduction at near room temperature and at high-pressure using an ionic liquid with a controlled concentration of water as electrolyte. A zinc sacrificial

anode was used and the experiment conditions were selected so that zinc electro-deposition at the cathode can be prevented or minimized.

This work also aims at exploring the benefits of using high-pressure, until now a scarcely studied process parameter. Namely high-pressure has the advantage of increasing the solubility of CO₂ in the ionic liquid-based electrolyte [7] helping to overcome mass transfer limitations. Another important advantage is that syngas can be obtained already at high-pressure reducing the costs of compression for posterior use and/or storage.

2. Experimental

2.1. Materials and reagents

Choline chloride HOC₂H₄N(CH₃)₃Cl[−] (ChCl) (Alfa Aesar >98% purity), urea (Sigma Aldrich 99.5% pa), anhydrous copper (II) chloride (Sigma Aldrich 99% purity), anhydrous zinc (II) chloride (Sigma Aldrich >98% purity), were used as received. 1-ethyl-3-methyl-imidazolium trifluoromethane sulfonate (triflate) (Iolitec >99% purity) was dried overnight before use. Its chemical structure is presented in Fig. 1.

Carbon dioxide from Air Liquide (N45 purity 99.995%) was used.

2.2. Electrodeposition of Zn–Cu coatings

The objective was to prepare bimetallic Zn–Cu cathodes by electro-deposition of Zn–Cu coatings on commercial copper foils of 1 mm thickness and ca. 1.2 cm² geometrical area. Two preparation methods were used, namely (i) co-deposition from the precursor metallic salts, and (ii) sequential deposition. Electro-depositions were carried out in a potentiostat/galvanostat EG&G Model 137 from Princeton Applied Research. A three-electrode system was employed. The working electrode was the catalytic cathode under study. The distance between working electrode and counter electrode was 13 mm. Prior to electro-deposition, the substrates were mechanically polished with 1200, 2500, silicon carbide emery paper and 3 μm and 1 μm emery cloth, thoroughly cleaned with distilled water, ethanol and then dried in air.

The plating baths were based on eutectic mixtures of choline chloride and urea. They were prepared by stirring the two components together, in the molar proportion ChCl:urea (1:2), at 70 °C until a homogeneous, colourless liquid was formed.

In the co-deposition method, 80 mM copper(II) chloride and 80 mM zinc(II) chloride were dissolved in ChCl:urea (1:2) and the deposition was carried out potentiostatically, at −0.5 V for 30 min, and at 60 °C. A platinum mesh was used as counter electrode and a Zn wire was used as quasi-reference electrode.

In the sequential deposition method, copper is first deposited on the copper foil substrate from a bath containing only the copper salt (200 mM) and then zinc is deposited from a second bath containing only the zinc salt (200 mM). A platinum mesh was used as counter electrode and a platinum wire was used as quasi-reference electrode. In this case, electro-depositions were carried out galvanostatically at 70 °C. The compositions of the electro-deposits were controlled by changing the current densities of

copper and zinc plating. The reproducibility of the cathode compositions was within 5%. After electro-deposition, the cathodes were thoroughly cleaned with distilled water, ethanol and then dried in air.

The performance of bimetallic Zn–Cu catalysts was also compared with the performance of catalysts consisting of copper particles deposited on the copper substrate and with catalysts consisting of zinc particles deposited on a commercial zinc foil substrate (ca. 1.2 cm² geometrical area) by the same method. The substrates were previously analysed by energy dispersive X-ray spectroscopy (EDS). No chemical elements were detected other than copper and zinc respectively.

2.2.1. Characterisation of Zn–Cu coatings

The crystalline structures of the coatings were determined by X-ray diffraction with a PANalytical X'Pert³ MRD, X-Ray diffractometer, with a Cu-Kα target. 2θ/θ scanning mode was executed in the range of 2θ = 20–100° with scan step size of 29.8 s and step size 2θ of 0.0167°.

Scanning electron microscopy (SEM) observations were carried out using a Carl Zeiss AURIGA CrossBeam (FIB–SEM) workstation coupled with energy dispersive X-ray spectroscopy (EDS) from Oxford Instruments. EDS was used to determine the surface elemental composition of the electro-deposits.

Atomic force microscopy (AFM) was used to evaluate the topography of the electrodeposits, employing an MFP-3D stand-alone Asylum Research instrument operated in tapping mode. Olympus AC160TS silicon probes attached to cantilevers with a nominal quality factor of 550 were used, with spring constant of 26.1 N m^{−1} and frequency resonance peak at 300 kHz. The scanning range was 85 × 85 μm², with a resolution of 256 × 256 lines.

2.3. Electrochemical experiments

2.3.1. Cyclic voltammetry

Cyclic voltammetry was carried out using an Autolab PGSTAT128N–Autolab 84469 potentiostat. A three-electrode system was used. The working electrode is made up of the catalytic material to be tested. A zinc anode and an Ag/Ag⁺ rod as a quasi-reference electrode (QRE) were used. All voltammograms were performed in a potential range from 0.1 V to −1.9 vs. reversible hydrogen electrode (RHE) at 45 °C, 30 bar pressure and a scan rate of 20 mV s^{−1}. The two first cycles were discarded. In the present work all potentials are reported with respect to RHE.

2.3.2. Electrolysis

The electrochemical reactor for CO₂ reduction consisted of an undivided electrochemical cell (see detailed description in Supplementary information). This cell used zinc, as a sacrificial anode, and an Ag/Ag⁺ rod as a quasi-reference electrode. The working electrode is made up of the catalytic material to be tested.

The electrolyte used was a mixture of the ionic liquid, 1-ethyl-3-methyl-imidazolium triflate (EMIMOTf) and water (10%wt.) contained in a glass beaker; 5 ml of EMIMOTf were used. The glass beaker with the electrodes and the electrolyte was housed inside a stainless-steel high-pressure vessel with an inner volume of approximately 150 cm³. This reactor can be operated in the temperature range from room temperature up to 80 °C, and work at pressures in the range of atmospheric- pressure up to 100 bar. After assembling the electrochemical reactor, CO₂ was introduced and removed repeatedly to remove air from the system. Then, carbon dioxide was brought to the desired pressure, and when the reactor stabilized at the desired temperature, current/potential was applied to the electrodes and electrolysis was carried out. A potentiostat/galvanostat PGSTAT128N–Autolab 84469 was used. Vacuum was applied to the sampling zone and the valves between

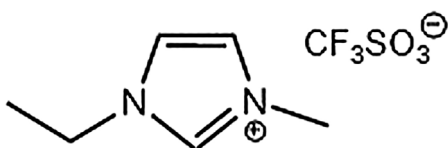


Fig. 1. Chemical structure of the ionic liquid 1-ethyl-3-methyl-imidazolium triflate (EMIMOTf).

the reactor and the sampling vessel were slowly opened until the pressure reached 2 bar in the sampling vessel and then closed. The sampling vessel was disconnected from the high-pressure facility and the gaseous mixture was analysed by gas chromatography.

Electrolysis were carried out under galvanostatic control with 10C, and 50C charge passed and under potentiostatic control at 50C charge passed.

2.4. Gas-phase analysis

Gaseous products were analysed by gas chromatography using a 3000 MicroGC from Agilent equipped with a thermal conductivity detector (TCD). Two columns were used, namely a molecular Sieve 5A, 10 m × 0.32 mm column with a Plot U 3 m × 0.32 mm pre-column with argon as carrier gas and Plot U 8 m × 0.32 mm column with Plot Q de 1 m × 0.32 mm as pre-column with helium as carrier gas. H₂, N₂, O₂, CO and CH₄ can be quantified in the molecular sieves column and CO₂ and higher hydrocarbons can be quantified with the Plot U column. Compositions were determined by comparison with calibrated gaseous mixtures of known compositions supplied by Air Liquide.

3. Results and discussion

3.1. Catalytic cathodes preparation and characterisation

A flexible process for the preparation of catalysts was developed that enables the preparation of a wide range of compositions from pure copper (0 at.% of zinc) up to pure zinc (100 at.% of Zn) yielding reproducible compositions and morphologies. This process can be used at an industrial scale, is environmentally friendly and energetically efficient. To achieve these goals deep eutectic solvents (DES) were chosen as solvents for the plating baths.

Electro-deposition in deep eutectic solvents/ILs plating baths has several advantages namely; it allows the preparation of “tailor-made” micro/nano-materials, by adjusting easily tunable parameters such as (i) voltage, (ii) current, (iii) bath composition and (iv) temperature. This process presents near 100% current efficiency due to absence of the competition of hydrogen evolution reaction, due to water electrolysis, always present in aqueous plating baths [27]. Aqueous plating baths often use complexing agents, as is the case of aqueous protocol for the electro-deposition of Zn–Cu alloys that employs cyanide salts, which pose serious environmental concerns. In his seminal work Barron [28] has shown that zinc-copper alloys could be electrodeposited from deep eutectic solvents, such as 1:2 choline chloride (ChCl):urea and 1:2 ChCl:ethylene glycol, on mild steel substrates. Bulk deposits were prepared from 1: 2 ChCl: urea and 1:2 ChCl:ethylene glycol, however, those deposited from 1:2 ChCl:urea were friable and non-adherent.

In this work zinc–copper alloys were electrodeposited on copper substrates from ChCl:urea plating baths showing good adhesion to the substrate and with a bright mirror-like surface. However, a limited range of compositions was obtained by co-deposition of copper and zinc in the conditions studied. Thus, a sequential deposition method was developed to widen the range of composition of bimetallic catalysts that could be prepared. In this method, by diffusion, the copper and zinc particles mix with each other giving rise to Zn–Cu alloys. One example of the morphology of one bimetallic Zn:Cu electro-deposit composition Zn:Cu 40:60 at.% obtained by co-deposition is presented in Fig. 2(a). This Figure also shows the characterization of this film of ca. 15 μm thickness by AFM, Fig. 2(b). Fig. 2(c) shows the cross section of the electro-deposit exhibiting a lamellar structure. This lamellar structure is common of electrodeposits obtained both by co-deposition and sequential deposition.

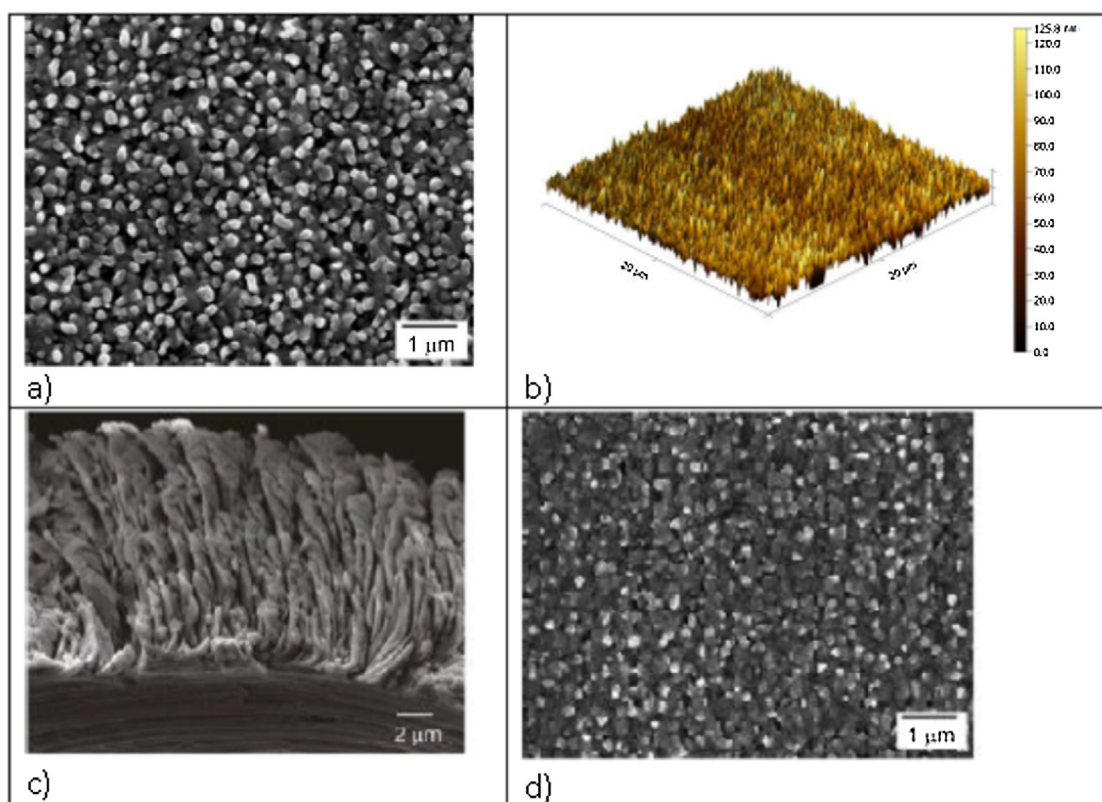


Fig. 2. Bimetallic cathode Zn:Cu (40:60) at.% (a) SEM image of the cathode obtained by co-deposition; (b) AFM analysis (c) SEM image of the cross-section of the cathode; (d) SEM image of the cathode Zn:Cu (40:60) obtained by sequential deposition.

Representative images of the bulk morphology of Zn–Cu deposits prepared by sequential deposition with varying Zn content are presented in Fig. 3. The deposits show a gradual change from the face-centered cubic (fcc) structure of pure copper to the hexagonal structure similar to pure zinc. The morphology of the electro-deposits was found to be independent of the electrolyte composition but strongly dependent on the relative composition of the deposit. This feature was also reported by Barron [28,29]. This can be observed, for example, when the morphology of a catalyst with a copper rich composition (40 at.% of Zn) obtained by co-deposition from a 80 mM Cu(II) and 80 mM Zn(II) plating bath of Fig. 2a is compared with the 40 at.% of zinc catalyst obtained by sequential deposition from 200 mM in Cu(II) and Zn(II) plating baths (Fig. 2d). In both cases the surface morphology exhibits polygonal appearance, irregular in shape. This observation is in accordance to the fact that electrodeposited copper-rich Zn–Cu alloys exhibit two phases: the α and β phases. The α phase is a solid solution that has an equilibrium solubility limit of about 35% Zn in Cu with a face-centered cubic (fcc) structure and the β phase has a body centered cubic structure [30]. The co-deposition of Zn–Cu has previously been demonstrated from an IL plating bath consisting in 50%–50% ZnCl₂:1-ethyl-3-methylimidazolium containing copper (I) on tungsten and nickel electrodes [31]. In this system a mixture of α and β phase Zn–Cu was also seen to form.

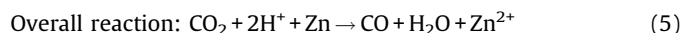
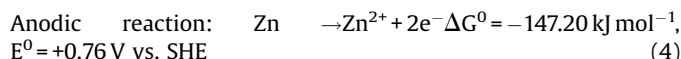
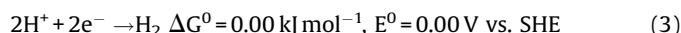
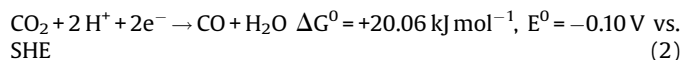
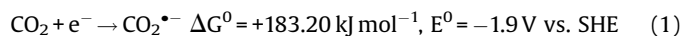
Fig. 4 shows X-ray diffraction (XRD) analysis of several Zn:Cu bimetallic cathodes prepared by sequential deposition. As the electro-deposits are relatively thin, all XRD spectra of Fig. 4 show an intense copper peak due to substrate contribution. For the composition (50:50) at.%, the presence of the phase Cu₅Zn₈ was identified. As the zinc content increases up to Zn:Cu (70:30) at.%, the content of the Cu₅Zn₈ phase increases in the coating in accordance with the phase diagram of Zn–Cu [30].

3.2. Electrochemical CO₂ reduction at high-pressure

In the system under study, syngas is produced by simultaneous reduction of protons at a bimetallic Zn–Cu cathode to yield hydrogen gas and reduction of CO₂ to yield CO at 30 bar and 45 °C. The pressure was selected to have a CO₂ solubility that was

experimentally determined to be 5.1 mmol CO₂/mL of electrolyte ca. ten times higher than CO₂ solubility at atmospheric pressure [32] by the method described in Zakrzewska et al. [33]. The temperature was selected to improve kinetics of the reaction and decrease the viscosity of the ionic liquid improving mass transfer [34].

The electrochemical reactions that are occurring are given below, together with the reaction Gibbs energy and theoretical equilibrium potential in standard conditions, 25 °C, atmospheric pressure, and for the reactions involving protons pH 0.



The composition of the electrolyte is 0.4 mol fraction of EMIMOTf and 0.6 mol fraction in water (10 wt.% of water in the electrolyte) i.e. the water content in the electrolyte is significant. Therefore, CO₂ will act both as a reagent and to a certain extent as a buffer, avoiding big shifts in the pH; the pH of the electrolyte before electrolysis was 5 and after electrolysis 6. Thus, the following equilibria should be considered:

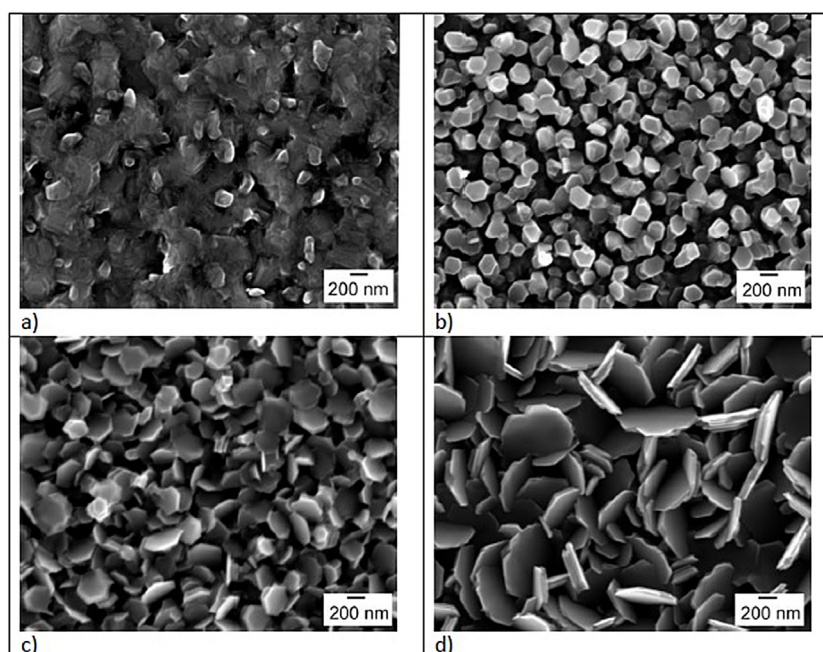
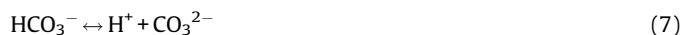
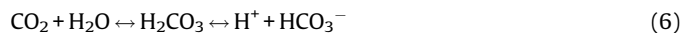


Fig. 3. SEM images of Zn:Cu bimetallic cathodes of ca. 4 cm² geometrical area. (a) Zn:Cu (30:70) at.%; (b) Zn:Cu (50:50) at.%; (c) Zn:Cu (70:30) at.%; (d) Zn:Cu (80:20) at.%.

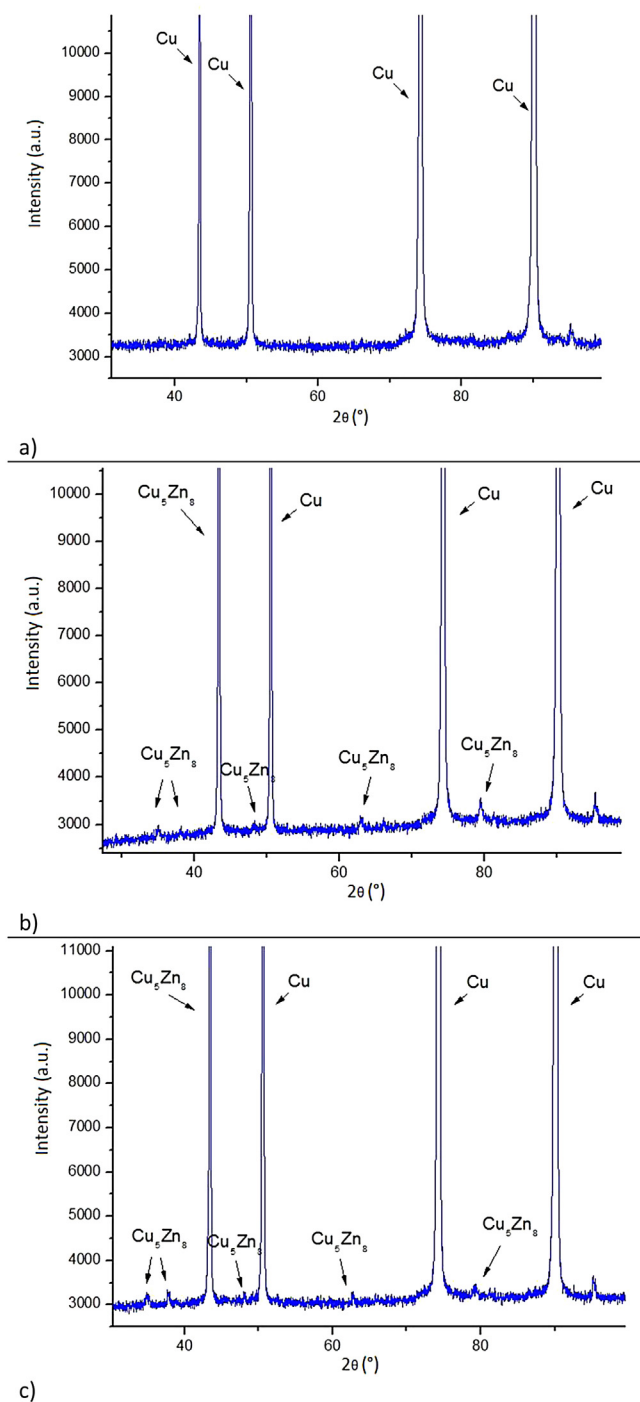


Fig. 4. XRD spectra of several compositions Zn:Cu bimetallic cathodes. (a) Zn:Cu (30:70) at.%, (b) Zn:Cu (50:50) at.%, (c) Zn:Cu (70:30) at.%.



When electrolyses were carried out, the formation of a white precipitate was observed. The precipitate was analysed by X-ray diffraction and the formation of zinc carbonate was confirmed (spectrum presented in Supplementary information). The formation of the precipitate of zinc carbonate helps to keep the concentration of zinc ions in the electrolyte low, so that the deposition of zinc at the cathode surface remains at residual levels when the total charge passed during electrolysis is low.

In the electrochemical experiments, current densities were calculated dividing the measured current values by the geometrical area of the electrodes.

3.3. Voltammetry study of CO₂ reduction

To have a stable electrochemical system, the ionic liquid must also be stable during electrolysis. The electrochemical stability window depends not only on the chemical structure of the materials used as electrolytes, but also of electrode materials, sweep rate of the potential, temperature, atmosphere, impurities etc. Since values of electrochemical windows in the literature have been evaluated under various conditions, it is not easy to compare these values. Ignat'ev et al. [35] reported a cathodic limit of -2.5 V vs. Ag/Ag⁺ (QRE) at atmospheric pressure of EMIMOTf 0.5 M solutions in CH₃CN at glassy carbon working electrode; auxiliary electrode was Pt and Ag/AgNO₃ (CH₃CN) was used as reference electrode. As the conditions used in this work are substantially different, the cathodic limit was evaluated in these conditions.

Cyclic voltammograms (CVs) in argon atmosphere were carried out to evaluate IL electrochemical stability and to define the baseline for cathode activity assessment. Thus, CVs with a copper cathode were obtained in the following conditions: dry 1-ethyl-3-methyl-imidazolium triflate (EMIMOTf) in a 30 bar argon atmosphere at 45 °C and in EMIMOTf with 10 wt.% H₂O in a 30 bar argon atmosphere at 45 °C. CVs were compared with those obtained in a 30 bar CO₂ atmosphere at 45 °C using copper, zinc and bimetallic Zn–Cu cathodes in EMIMOTf with 10 wt.% H₂O. Water content of EMIMOTf after the drying procedure was determined by Karl-Fischer titration, typically 0.14 wt.%. The relationship between voltage and current density in these conditions, for a copper, zinc and for a bimetallic cathode with a composition of Zn:Cu (70:30) at.%, representing a typical CV of a bimetallic Zn–Cu cathode, is depicted in Fig. 5. The inset Figure shows more clearly the potentials of onset currents and for simplicity's sake only the cathodic curves are presented. Cathodic curves without defined peaks were obtained, similar to the ones reported by Lau et al. at 100 mV s⁻¹ [36]. When the scan is reversed into the anodic direction, anodic peak currents were observed for the bimetallic and zinc cathodes at potentials less negative than -0.3 V vs. RHE – zinc open circuit potential in the system under study – that appear to be related to zinc oxidation.

The cathodic limit in the CV of the previously dried EMIMOTf, in the aforementioned conditions, and onset potential of electrochemical reactions were evaluated considering a cut-off current of -1 mA cm⁻² [27]. The cathodic curve of the copper cathode in a 30 bar argon atmosphere shows for the dried IL a current increase at -1.2 V vs. RHE due most probably to the reduction of the protons of water still present in the IL. With the addition of 10 wt.% water to the electrolyte, an onset potential is evident at -0.8 V vs. RHE as well as a steep current increase at a potential of ca. -1.2 V vs. RHE attributed to the onset of proton reduction and to the limiting current for hydrogen evolution, respectively.

The data presented in Fig. 5 shows that the ionic liquid is electrochemically stable, at least in the potential range of -1.2 V up to 0.1 V vs. RHE. Samples of electrolytes submitted to electrolysis carried out at potentials of ca. -1.4 V vs. RHE and even slightly more negative were analysed by ¹H NMR in D₂O with water suppression. No ionic liquid decomposition was observed at these more negative potentials (spectra presented in Supplementary information).

In a 30 bar CO₂ atmosphere, the cathodic curve corresponding to the zinc and copper cathode in EMIMOTf with 10 wt.% water electrolyte show a significant shift towards more positive potentials and a steep current increase at a potential of ca. -0.4 V vs. RHE, and of ca. -0.3 V vs. RHE, respectively. This is

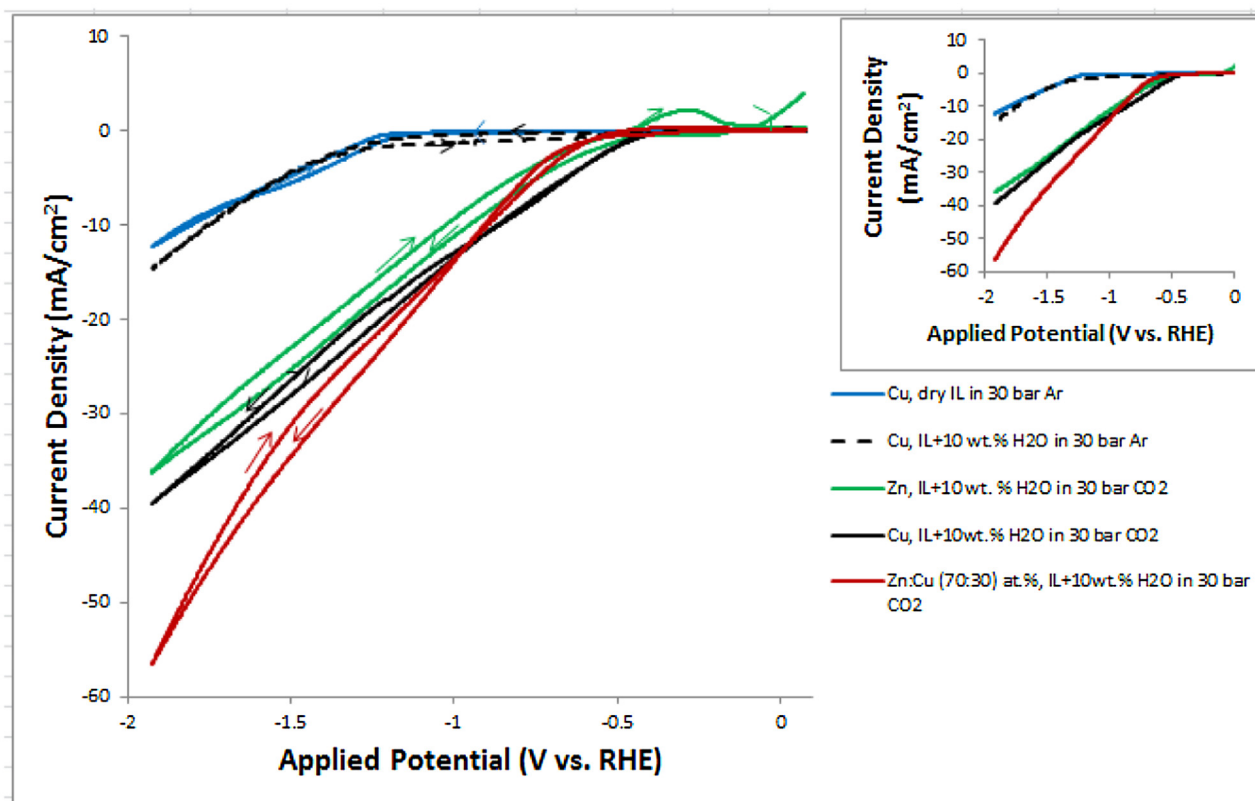


Fig. 5. Cyclic voltammograms of catalytic cathodes at 45 °C and 30 bar, carried out at 20 mV s⁻¹ in the potential range of 0.1 V to -1.9 V vs. RHE. black curve—copper cathode in dry EMIMOTf in an argon atmosphere, dashed black curve—copper cathode in EMIMOTf with 10 wt.% H₂O in an argon atmosphere, green curve—zinc cathode in EMIMOTf with 10 wt.% H₂O in a CO₂ atmosphere, blue curve—copper cathode in EMIMOTf with 10 wt.% H₂O in a CO₂ atmosphere and brown curve—bimetallic Zn–Cu (70:30) at.% cathode in EMIMOTf with 10 wt.% H₂O in a CO₂ atmosphere. (For interpretation of the references to colour in this figure legend, the reader is referred to the web version of this article.)

attributed to the onset of CO₂ reduction. The relationship between onset potentials and cathode composition (CVs other than those reported in Fig. 5 are not shown) is presented in Fig. 6a). Current densities for an applied potential of -0.9 V vs. RHE, are plotted in Fig. 6b). It can be observed that onset potentials shift slightly to more negative values for bimetallic cathodes, when compared with the pure metals. Current densities are approximately the same for the whole range of cathode compositions studied for an applied potential of -0.9 V vs. RHE.

3.4. Activity and selectivity of Zn–Cu bimetallic cathodes

The H₂ and CO (millimoles) produced in 10C electrolysis, carried out under galvanostatic control, and 50C electrolysis, carried out under potentiostatic control, determined by gas chromatography are presented in Fig. 7a and b, respectively. The number of millimoles indicated is an average of three or four measurements. For 10C electrolysis the average standard deviations are 30% and 40% for H₂ and CO, respectively, as the sensitivity of the TCD detector is lower for CO than for hydrogen (see Supplementary information). In potentiostatic 50C electrolysis, in the range of compositions studied, the amount of CO produced is higher,

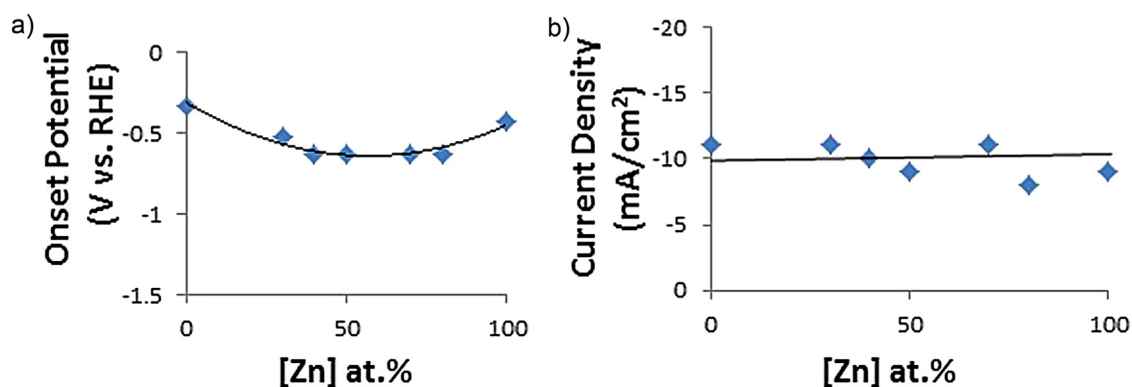


Fig. 6. (a) Onset potentials vs. cathode composition (b) current densities for an applied potential of -0.9 V vs. RHE.

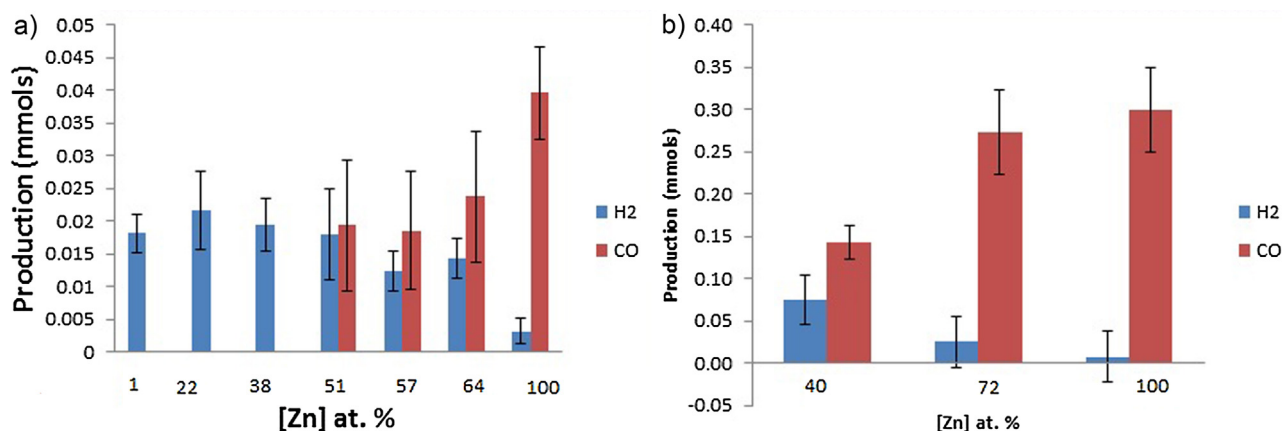


Fig. 7. Millimoles of H₂ and CO produced at 30 bar CO₂ and 45 °C vs. composition of bimetallic Zn–Cu catalysts of (a) 10C electrolysis carried out in the galvanostatic mode (–6 mA applied current); (b) 50C electrolysis carried out in potentiostatic mode at –0.8 V applied potential vs. RHE at 30 bar CO₂ and 45 °C. The bars represent standard deviations.

leading to an average standard deviation for CO of 20%. As the quantities of hydrogen produced are very small, the average standard deviation of H₂ is in this case significantly higher, 53%.

In 50C electrolysis as the concentration of zinc ions in solution increases, zinc deposition on the cathode becomes significant. Thus, data is only presented for cathodes with a variation of the composition, before and after the electrolysis, of less than 15%, corresponding to zinc compositions higher than 40%, where it is expected low amounts of hydrogen produced. However, in this case, the average standard deviation for CO of 20% is much lower showing that the sensitivity of the detector is determinant.

From the observation of this figure it is clearly evident that in the conditions studied only the bimetallic cathodes are significantly active for syngas.

Faradaic efficiency (FE) is a measure of the selectivity of the electrochemical reaction and is calculated according to equation 9, by the ratio of the equivalent current of the product formed by the current passed during electrolysis, where j_i is the partial current of the product i and $|j_{total}|$ the current passed during electrolysis. The partial currents for each product were estimated by the quantities of products produced in the electrolysis determined by gas chromatography as described in detail in Supplementary information. As gaseous products, only hydrogen and carbon monoxide were detected. In Fig. 8 is plotted total Faradaic efficiency (Total FE) vs. cathode composition. It can be observed

that the selectivity for the gaseous products increases with increasing zinc content of the cathode, reaching a value near 100% for a zinc cathode. The significantly lower than 100% total Faradaic efficiencies exhibited by the copper rich cathodes compositions, can most probably be explained by the formation of liquid products that is not addressed in this work. It has been observed by several researchers that copper cathodes could reduce CO₂ into a wide range of liquid products (at room temperature and atmospheric pressure) including aldehydes, ketones, alcohols, and carboxylic acids using aqueous electrolytes [37–39].

As this work addresses only the study of gaseous products, normalized Faradaic efficiencies (NFE) were calculated according to Eq. (10), where j_i is the partial current of the gaseous product CO, or H₂ divided by the summation of CO and H₂ estimated partial currents.

$$\text{Total FE}(\%) = \frac{j_i}{|j_{total}|} \times 100 \quad (9)$$

$$\text{NFE}(\%) = \frac{j_i}{j_{CO} + j_{H_2}} \times 100 \quad (10)$$

Fig. 8 also depicts normalized Faradaic efficiencies versus the composition of bimetallic Zn–Cu catalysts of 10C and 50C electrolyses carried out in galvanostatic mode (–6 mA applied current) at 30 bar CO₂ and 45 °C. Fig. 8 shows that in 10C electrolysis for zinc compositions near 40%, CO starts to be produced. When the content of zinc increases, Faradaic efficiency of hydrogen drops nearly to zero for pure zinc. CO Faradaic efficiencies increase steadily until a Faradaic efficiency of approx.

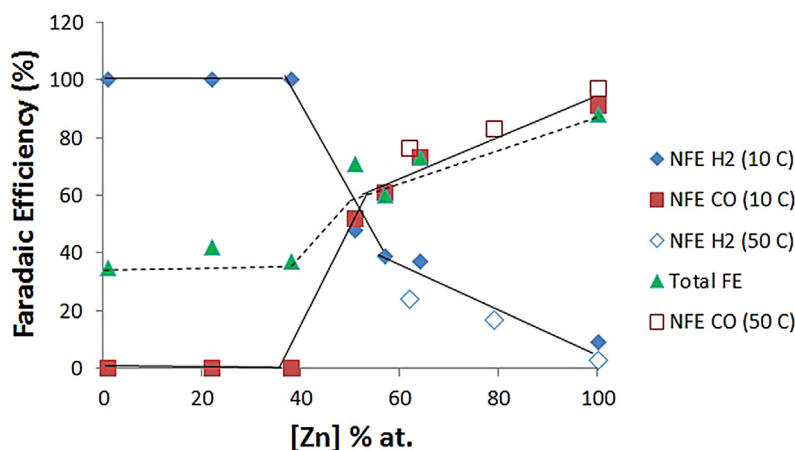


Fig. 8. Faradaic efficiencies vs. composition of bimetallic Zn–Cu cathodes of 10C and 50C electrolysis carried out in galvanostatic mode at –6 mA/cm² applied current at 30 bar CO₂ and 45 °C.

100% is reached for pure zinc. For 50C electrolysis a similar trend is observed for compositions higher than 60 at.% of zinc.

Electrolysis were also carried out in potentiostatic mode at -0.8 V applied potential vs. RHE at 30 bar CO₂ and 45 °C and 50C charge passed. Current densities during electrolysis varied typically in the range of 2–13 mA/cm². Faradaic efficiencies vs. composition of bimetallic cathodes are plotted in Fig. 9. In these conditions, an approximate linear increase in the Faradaic efficiencies of CO produced is observed as the content in zinc increases, while the Faradaic efficiency for hydrogen decreases. In this range of cathode compositions the same trend is observed for electrolysis carried out both under galvanostatic and potentiostatic control.

Table 1 summarizes the results of Figs. 7–9. The values of total faradaic efficiencies higher than 100% for zinc cathodes or zinc rich compositions are within the experimental error.

Figs. 7 and 8 show two types of behaviours. For copper rich compositions the electrochemical reaction is controlled by copper and in the conditions studied no CO was detected. When the content of zinc is higher than 40 at.% of zinc, CO starts to be produced and zinc starts to control the electrochemical reaction. This work is in accordance with the work of Katoh et al. [26] in which it was reported that the Cu₅Zn₈ phase promotes the formation of CO. This is precisely the range of compositions in which the content of the Cu₅Zn₈ phase starts to increase. In the range 40 at.% of zinc–pure zinc selectivities for the gaseous product, syngas near 100% are obtained. Chromatograms of the analysis of gaseous products are presented in the Supplementary information. For compositions higher than 60 at.% of zinc, Faradaic efficiencies are the same within experimental error for 10C and 50C electrolysis. This trend indicates that the ratio H₂/CO is controlled by the electrode composition and not by the duration of the electrolysis. As mentioned in the Experimental section, the catalysts composition is determined by EDS. When the electron beam hits the surface of the sample, it penetrates the sample to a depth of a few microns. The estimated composition is the average composition of the volume of interaction between the electronic beam and the sample. Although it could be argued the method of catalyst preparation yields a gradient in zinc concentrations decreasing from the surface to the copper substrate, diffusion among copper and zinc particles promotes alloying between the two metals and the average composition determined by EDS correlates with the surface composition “seen” by protons and CO₂ interacting at the electrode’s surface. The operation at high pressure promotes the formation of the CO₂–CO₂^{•-} dimer, due to

Table 1

Production of gaseous products and faradaic efficiencies of (a) galvanostatic electrolysis and (b) potentiostatic electrolysis.

Galvanostatic electrolysis (-6 mA applied current)						
Composition [Zn] at. %	Charge (C)	H ₂ (mmols)	CO (mmols)	NFEH ₂ (%)	NFECO (%)	Total FE (%)
<1	10	0.018	n.d.	100	–	35
22 ± 5	10	0.022	n.d.	100	–	42
38 ± 5	10	0.019	n.d.	100	–	37
51 ± 5	10	0.018	0.019	48	52	71
57 ± 5	10	0.012	0.019	39	61	60
62 ± 5	50	0.060	0.188	24	76	96
64 ± 5	10	0.014	0.024	37	73	73
79 ± 15	50	0.007	0.273	17	83	108
100	10	0.003	0.040	7	93	83
100	50	0.009	0.289	3	97	115
Potentiostatic electrolysis (-0.8 V vs. RHE)						
40 ± 15	50	0.075	0.144	34	66	85
72 ± 15	50	0.025	0.273	8	92	115
100	50	0.008	0.299	3	97	118

n.d.—non detected.

the increased CO₂ concentration in solution [40]. This species is stable even in the gas phase and has a positive electron affinity (+0.9 eV), compared to a negative value for CO₂^{•-} itself (–0.6 eV) [41]. This leads to the prediction that the dimer radical could be as much as 1.5 eV easier to be formed electrochemically than the simple radical. According to Fig. 7(a) considering an average onset potential of CO₂ reduction of -0.6 V vs. RHE in the range of compositions, which yield syngas, this represents a 1.3 V positive shift in respect of the reversible potential for the CO₂/CO₂^{•-} couple.

The impressive shift to more positive potentials in the cathodic curve of Fig. 6 corresponding to EMIMOTf with 10 wt.% water electrolyte in a 30 bar CO₂ atmosphere illustrates the catalytic effect of the couple catalytic cathode/electrolyte lowering the overpotential of this reaction. Recently, the role of co-catalyst in the electrochemical reduction CO₂ of the imidazolium cations has been explained through the stabilization of the CO₂^{•-} intermediary by their C-4 and C-5 protons [36].

Based on the production values presented in Fig. 7(a) the electrode yield can be calculated. Considering e.g. a syngas composition H₂:CO (1:1) yields of 85 NμL cm⁻² C⁻¹/170 NμL cm⁻² h⁻¹ were obtained, where N stands for volume at “normal” conditions, 0 °C and atmospheric pressure.

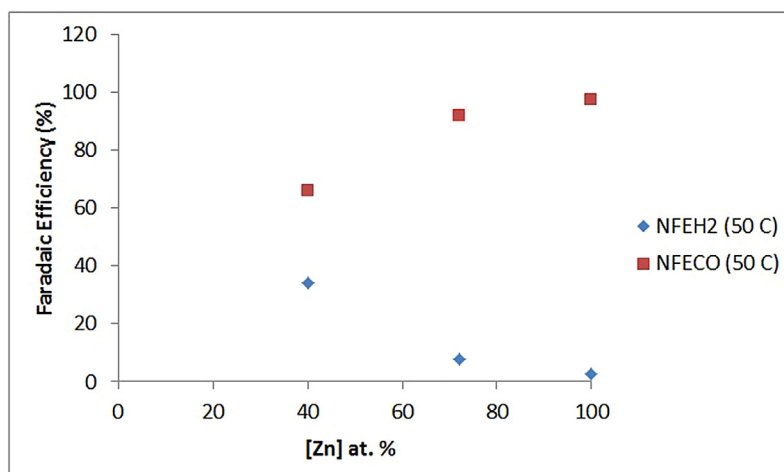


Fig. 9. Normalized Faradaic efficiencies vs. composition of bimetallic Zn–Cu cathodes of 50C electrolysis carried out in potentiostatic mode at -0.8 V applied potential vs. RHE at 30 bar CO₂ and 45 °C.

4. Conclusions

In this work the development of an innovative technology to produce low carbon footprint syngas, an industrially important chemical building block at high-pressure, is reported.

The novelty of the process is the use of the catalytic couple Zn–Cu bimetallic cathode/ionic-based electrolyte that allows tuning the H₂/CO ratio by the choice of the composition of the developed catalyst. The significance of these results lies in the fact that most of the processes for syngas production yield either a fixed H₂/CO ratio or offer very limited tunability, making it more difficult and costly to achieve the optimum ratios necessary for the production of the different chemical products that can be obtained from syngas.

With syngas gaseous mixtures selectivity's being nearly 100% (for Zn concentrations higher than 40 at.%) and with negligible solubility in the electrolyte, the process under development avoids complex and costly purification procedures.

These features suggest that this electrochemical technology based on cathodes made-up of common metals can be developed into a commercial process. To achieve this goal, two approaches are being carried out: (i) replacement of the sacrificial anode, not an option for a commercial process, by one of the many commercial anodes available in the market, optimized for oxygen evolution in aqueous media. (ii) optimization of electrochemical reactor configuration. In the configuration currently under study, a cathodic compartment is separated from the anodic compartment by a protonic exchange membrane. The design of the reactor is being optimized to allow reactor operation in semi-continuous or continuous mode to overcome mass transport issues derived from batch mode operation. This work leverages on the knowledge available concerning the design of electro-catalytic reactors in the field of hydrogen fuel cells/electrolysers [42–44].

Scale-up of the catalytic cathodes implies higher geometrical and electrochemical surface area electrodes, of the order of 10⁹ cm², similar to those in commercial electrochemical cells for the chlorine-alkali process.

In order to produce a fully carbon neutral cycle, it is envisaged to use waste CO₂ captured from industrial emissions, stored and/or transported at high-pressure, for electrochemical conversion using the technology under development powered by renewable energy.

Acknowledgements

We thank Tomás Calmeira for the AFM analysis.

This work was supported by the 7th Framework Program under the project CEOPS (FP7-NMP-2012-309984), by the European Regional Development Funds QREN Mais Centro -07-0202-FEDER-030145 and by the Associate Laboratory Research Unit for Green Chemistry – Technologies and Processes Clean – LAQV which is supported by national funds from FCT/MEC (UID/QUI/50006/2013) and co-financed by the ERDF under the PT2020 Partnership Agreement (POCI-01-0145-FEDER-007265).

Appendix A. Supplementary data

Supplementary data associated with this article can be found, in the online version, at <http://dx.doi.org/10.1016/j.jcou.2017.01.007>.

References

- [1] F. Jiao, J. Li, X. Pan, J. Xiao, H. Li, H. Ma, M. Wei, Y. Pan, Z. Zhou, M. Li, S. Miao, J. Li, Y. Zhu, D. Xiao, T. He, J. Yang, F. Qi, Q. Fu, X. Bao, Selective conversion of syngas to light olefins, *Science* 351 (2016) 1065–1068, doi:<http://dx.doi.org/10.1126/science.aaf1835>.
- [2] T.V. Choudhary, V.R. Choudhary, Energy-efficient syngas production through catalytic oxy-methane reforming reactions, *Angew. Chemie Int. Ed.* 47 (2008) 1828–1847, doi:<http://dx.doi.org/10.1002/anie.200701237>.
- [3] F. Wang, L. Xu, W. Shi, Syngas production from CO₂ reforming with methane over core-shell Ni@SiO₂ catalysts, *J. CO₂ Util.* 16 (2016) 318–327, doi:<http://dx.doi.org/10.1016/j.jcou.2016.09.001>.
- [4] K. Chandrasekaran, L.O. Bockris, In-situ spectroscopic investigation of adsorbed intermediate radicals in electrochemical reactions: CO₂-on platinum, *Surf. Sci.* 185 (1987) 495–514, doi:[http://dx.doi.org/10.1016/S0039-6028\(87\)80173-5](http://dx.doi.org/10.1016/S0039-6028(87)80173-5).
- [5] J.P. Jones, G.K.S. Prakash, G.A. Olah, Electrochemical CO₂ reduction: recent advances and current trends, *Isr. J. Chem.* 54 (2014) 1451–1466, doi:<http://dx.doi.org/10.1002/ijch.201400081>.
- [6] G. Zhao, T. Jiang, B. Han, Z. Li, J. Zhang, Z. Liu, J. He, W. Wu, Electrochemical reduction of supercritical carbon dioxide in ionic liquid 1-n-butyl-3-methylimidazolium hexafluorophosphate, *J. Supercrit. Fluids* 32 (2004) 287–291, doi:<http://dx.doi.org/10.1016/j.supflu.2003.12.015>.
- [7] L.A. Blanchard, D. Hancu, E.J. Beckman, J.F. Brennecke, Green processing using ionic liquids and CO₂, *Nature* 399 (1999) 28–29, doi:<http://dx.doi.org/10.1038/19887>.
- [8] L.E. Barrosse-Antle, R.G. Compton, Reduction of carbon dioxide in 1-butyl-3-methylimidazolium acetate, *Chem. Commun. (Camb)* (2009) 3744–3746, doi:<http://dx.doi.org/10.1039/b906320j>.
- [9] J.L. DiMaggio, J. Rosenthal, Selective conversion of CO₂ to CO with high efficiency using an inexpensive bismuth-based electrocatalyst, *J. Am. Chem. Soc.* 135 (2013) 8798–8801, doi:<http://dx.doi.org/10.1021/ja4033549>.
- [10] J. Medina-Ramos, R.C. Pupillo, T.P. Keane, J.L. DiMaggio, J. Rosenthal, Efficient conversion of CO₂ to CO using tin and other inexpensive and easily prepared post-transition metal catalysts, *J. Am. Chem. Soc.* 137 (2015) 5021–5027, doi:<http://dx.doi.org/10.1021/ja5121088>.
- [11] M. Alvarez-Guerra, J. Albo, E. Alvarez-Guerra, A. Irabien, Ionic liquids in the electrochemical valorisation of CO₂, *Energy Environ. Sci.* 8 (2015) 2574–2599, doi:<http://dx.doi.org/10.1039/C5EE01486G>.
- [12] B.A. Rosen, A. Salehi-Khojin, M.R. Thorson, W. Zhu, D.T. Whipple, P.J.A. Kenis, R. I. Masel, Ionic liquid-mediated selective conversion of CO₂ to CO at low overpotentials, *Science* 334 (2011) 643–645.
- [13] Z. Zhang, M. Chi, G.M. Veith, P. Zhang, D.A. Lutterman, J. Rosenthal, S.H. Overbury, S. Dai, H. Zhu, Rational design of Bi nanoparticles for efficient electrochemical CO₂ reduction: the elucidation of size and surface condition effects, *ACS Catal.* 6 (2016) 6255–6264, doi:<http://dx.doi.org/10.1021/acscatal.6b01297>.
- [14] J.D. Watkins, A.B. Bocarsly, Direct reduction of carbon dioxide to formate in high-gas-capacity ionic liquids at post-transition-metal electrodes, *ChemSusChem* 7 (2014) 284–290, doi:<http://dx.doi.org/10.1002/cssc.201300659>.
- [15] L. Sun, G.K. Ramesha, P.V. Kamat, J.F. Brennecke, Switching the reaction course of electrochemical CO₂ reduction with ionic liquids, *Langmuir* 30 (2014) 6302–6308.
- [16] N. Hollingsworth, S.F.R. Taylor, M.T. Galante, J. Jacquemin, C. Longo, K.B. Holt, N. H. De Leeuw, C. Hardacre, Reduction of carbon dioxide to formate at low overpotential using a superbase ionic liquid, *Angew. Chem. Int. Ed.* 54 (2015) 14164–14168, doi:<http://dx.doi.org/10.1002/anie.201507629>.
- [17] C. Wang, X. Luo, H. Luo, D.E. Jiang, H. Li, S. Dai, Tuning the basicity of ionic liquids for equimolar CO₂ capture, *Angew. Chem. Int. Ed.* 50 (2011) 4918–4922, doi:<http://dx.doi.org/10.1002/anie.201008151>.
- [18] M. Asadi, K. Kim, C. Liu, A.V. Addepalli, P. Abbasi, Y. Poya, A. Behranginia, P. Phillips, J.M. Cerrato, R. Haasch, P. Zapol, B. Kumar, R.F. Klie, J. Abiade, L.A. Curtiss, A. Alehi-Khojin, Robust carbon dioxide reduction on molybdenum disulphide edges, *Nat. Commun.* 5 (2014) 1330–1333, doi:<http://dx.doi.org/10.1038/ncomms5470>.
- [19] Z. Liu, R.I. Masel, Q. Chen, R. Kutz, H. Yang, K. Lewinski, M. Kaplun, S. Luopa, D.R. Lutz, Electrochemical generation of syngas from water and carbon dioxide at industrially important rates, *J. CO₂ Util.* 15 (2016) 50–56, doi:<http://dx.doi.org/10.1016/j.jcou.2016.04.011>.
- [20] B.A. Rosen, J.L. Haan, P. Mukherjee, B. Braunschweig, W. Zhu, A. Salehi-Khojin, D.D. Dlott, R.I. Masel, In situ spectroscopic examination of a low overpotential pathway for carbon dioxide conversion to carbon monoxide, *J. Phys. Chem. C* 116 (2012) 15307–15312, doi:<http://dx.doi.org/10.1021/jp210542v>.
- [21] Y. Hori, Electrochemical CO₂ reduction on metal electrodes, in: C.G. Vayenas, R. E. White, M.E. Gamboa-Aldeco (Eds.), *Mod. Asp. Electrochem.*, Springer, New York, 2008, pp. 89–189, doi:http://dx.doi.org/10.1007/978-0-387-49489-0_3.
- [22] K.H. Hiejima, Y. Hayashi, M. Uda, A. Oya, S.K. Senboku, H. Takahashi, Electrochemical carboxylation of *a*-chloroethylbenzene in ionic liquids compressed with carbon dioxide, *Phys. Chem. Chem. Phys.* 12 (2010) 1953–1957.
- [23] K. Hara, T. Sakata, Electrochemical reduction of high pressure carbon dioxide on a gold electrode on phosphate buffer solutions, *Bull. Chem. Soc. Jpn.* 70 (1997) 571–576.
- [24] R.M. Ormerod, Solid oxide fuel cells, *Chem. Soc. Rev.* 32 (2003) 17–28, doi:<http://dx.doi.org/10.1039/b105764m>.
- [25] J. Hallinder, P. Holtappels, M. Mogensen, Electrochemical reduction of CO, *ECS Trans.* 41 (2012) 61–73, doi:<http://dx.doi.org/10.1149/1.3702413>.
- [26] A. Katoh, H. Uchida, M. Shibata, M. Watanabe, Design of electrocatalyst for CO₂ reduction, *J. Electrochem. Soc.* 141 (1994) 2054, doi:<http://dx.doi.org/10.1149/1.2055059>.

- [27] F. Endres, Douglas MacFarlane, Andrew Abbott, *Electrodeposition from Ionic Liquids*, Wiley-VCH, 2008.
- [28] J.C. Barron, *The electrochemistry of zinc in deep eutectic solvents*, PhD Thesis, University of Leicester, 2009.
- [29] A.P. Abbott, J.C. Barron, K.S. Ryder, Electrolytic deposition of Zn coatings from ionic liquids based on choline chloride, *Trans. IMF* 87 (2009) 201–207, doi: <http://dx.doi.org/10.1179/174591909X438857>.
- [30] K. Hansen, M. Anderko, *Constitution of Binary Alloys*, McGraw-Hill, New York, 1958.
- [31] P.-Y. Chen, M.C. Lin, I.W. Sun, Electrodeposition of Cu-Zn alloy from a Lewis acidic ZnCl₂-EMIC molten salt, *J. Electrochem. Soc.* 147 (2000) 3350–3355.
- [32] M. Zakrzewska, M. Nunes da Ponte, **To be published.**
- [33] M. Zakrzewska, M. Nunes da Ponte, Volumetric and phase behaviour of mixtures of fluoroalkylphosphate-based ionic liquids with high pressure carbon dioxide, *J. Supercrit. Fluids* 113 (2016) 61–65, doi: <http://dx.doi.org/10.1016/j.supflu.2016.03.017>.
- [34] O.O. Okoturo, T.J. VanderNoot, Temperature dependence of viscosity for room temperature ionic liquids, *J. Electroanal. Chem.* 568 (2004) 167–181, doi: <http://dx.doi.org/10.1016/j.jelechem.2003.12.050>.
- [35] N.V. Ignat'ev, P. Barthen, A. Kucheryna, H. Willner, P. Sartori, A convenient synthesis of triflate anion ionic liquids and their properties, *Molecules* 17 (2012) 5319–5338, doi: <http://dx.doi.org/10.3390/molecules17055319>.
- [36] G.P.S. Lau, M. Schreier, D. Vasilyev, R. Scopelliti, M. Grätzel, P.J. Dyson, New insights into the role of imidazolium-based promoters for the electroreduction of CO₂ on a silver electrode, *J. Am. Chem. Soc.* 138 (2016) 7820–7823, doi: <http://dx.doi.org/10.1021/jacs.6b03366>.
- [37] K.P. Kuhl, E.R. Cave, D.N. Abram, T.F. Jaramillo, New insights into the electrochemical reduction of carbon dioxide on metallic copper surfaces, *Energy Environ. Sci.* 5 (2012) 7050–7059, doi: <http://dx.doi.org/10.1039/c2ee21234j>.
- [38] C.W. Li, J. Ciston, M.W. Kanan, Electroreduction of carbon monoxide to liquid fuel on oxide-derived nanocrystalline copper, *Nature* 508 (2014) 504–507, doi: <http://dx.doi.org/10.1038/nature13249>.
- [39] E. Bertheussen, A. Verdager-Casadevall, D. Ravasio, J.H. Montoya, D.B. Trimarco, C. Roy, S. Meier, J. Wendland, J.K. Nørskov, I.E.L. Stephens, I. Chorkendorff, Acetaldehyde as an intermediate in the electroreduction of carbon monoxide to ethanol on oxide-derived copper, *Angew. Chem. Int. Ed.* 55 (2016) 1450–1454, doi: <http://dx.doi.org/10.1002/anie.201508851>.
- [40] A. Gennaro, I. Bhugunb, J. Saveant, Mechanism of the electrochemical reduction of carbon dioxide at inert electrodes in media of low proton availability, *J. Chem. Soc. Faraday Trans.* 92 (1996) 3963–3968.
- [41] D.A. Tryk, A. Fujishima, Electrochemists enlisted in war, the carbon dioxide reduction battle, *Electrochem. Soc. Interface* (2001) 32–36.
- [42] J.K.E. Ayers, E.B. Anderson, C.B. Capuano, B.D. Carter, L.T. Dalton, G. Hanlon, J. Manco, M. Niedzwiecki, Advances towards low cost, high efficiency PEM electrolysis, *ECS Trans.* 33 (2010) 3–15.
- [43] M. Carmo, D.L. Fritz, J. Mergel, D. Stolten, A comprehensive review on PEM water electrolysis, *Int. J. Hydrogen Energy* 38 (2013) 4901–4934, doi: <http://dx.doi.org/10.1016/j.ijhydene.2013.01.151>.
- [44] C. Xiang, K.M. Papadantonakis, N.S. Lewis, Principles and implementations of electrolysis systems for water splitting, *Mater. Horiz.* 3 (2016) 169–173, doi: <http://dx.doi.org/10.1039/c6mh00016a>.